MATHEMATICAL BIOSCIENCES
AND ENGINEERING
Volume **1**, Number **1**, June **2004**

http://math.asu.edu/~mbe/

pp. **185–211**

NOISE IN ECOSYSTEMS: A SHORT REVIEW

B. Spagnolo, D. Valenti, A. Fiasconaro

Dipartimento di Fisica e Tecnologie Relative
Istituto Nazionale di Fisica della Materia, Unità di Palermo
Università di Palermo
Viale delle Scienze, I-90128 Palermo, Italy

(Communicated by Stefano Boccaletti)

Abstract. Noise, through its interaction with the nonlinearity of the living systems, can give rise to counter-intuitive phenomena such as stochastic resonance, noise-delayed extinction, temporal oscillations, and spatial patterns. In this paper we briefly review the noise-induced effects in three different ecosystems: (i) two competing species; (ii) three interacting species, one predator and two preys, and (iii) N-interacting species. The transient dynamics of these ecosystems are analyzed through generalized Lotka-Volterra equations in the presence of multiplicative noise, which models the interaction between the species and the environment. The interaction parameter between the species is random in cases (i) and (iii), and a periodical function, which accounts for the environmental temperature, in case (ii). We find noise-induced phenomena such as quasi-deterministic oscillations, stochastic resonance, noise-delayed extinction, and noise-induced pattern formation with non-monotonic behaviors of patterns areas and of the density correlation as a function of the multiplicative noise intensity. The asymptotic behavior of the time average of the i^{th} population when the ecosystem is composed of a great number of interacting species is obtained and the effect of the noise on the asymptotic probability distributions of the populations is discussed.

1. **Introduction.** In recent years several theoretical investigations have been done on noise-induced effects in population dynamics [1]-[8]. In particular, the problem of the stability of complex ecological systems in the presence of noise has been widely discussed [9]. New counterintuitive phenomena, such as stochastic resonance [10, 11], noise enhanced stability [12] and noise delayed extinction [6, 13, 14], can appear because of the presence of noise in living systems, whose dynamics is nonlinear. The interaction between noise and nonlinear determinism in ecological dynamics adds an extra level of complexity compared with the largely stochastic dynamics of, say, economic systems or the largely deterministic dynamics of many physical and chemical processes [15]. Ecological systems are open systems in which the interaction between the component parts is nonlinear and the interaction with the environment is noisy. This intrinsic nonlinearity can give rise to the complex behavior of the system, which becomes very sensitive to initial conditions, various

2000 *Mathematics Subject Classification.* PACS: 05.40.-a, 87.23.Cc, 89.75.Kd, 87.23.-n
82Cxx:Time-dependent statistical mechanics (dynamic and nonequilibrium),
92Dxx:92D25 Population dynamics (general).

Key words and phrases. Nonequilibrium Statistical Mechanics, Population Dynamics, Noise-induced effects,
Spatio-Temporal Patterns.

Research supported by INTAS Grant 01-450, by MIUR and INFM.

deterministic external perturbations, and to fluctuations always present in nature. The comprehension of noise's role in the dynamics of nonlinear systems plays a key aspect in the efforts devoted to understand and then to model so-called complex ecosystems. One approach to understanding the complexity is to start with a conceptually simple view of the system in order to catch the phenomena of interest and then to add details that introduce new levels of complexity [9, 16]. In general the effects of small perturbations and noise, which are ubiquitous in real systems, can be quite difficult to predict and often yield counterintuitive behavior. Even low-dimensional systems exhibit a huge variety of noise-driven phenomena, ranging from a less ordered to a more ordered system dynamics.

In the past, the study of deterministic mathematical models of ecosystems has clearly revealed a large variety of phenomena, ranging from deterministic chaos to the presence of a spatial organization. These models, however, do not account for the effects of noise despite the facts that it is always present in actual population dynamics and that it arises from different sources, such as the intrinsic stochasticity associated with the random variability of the environment. Frequently, its effects have been assumed to be only a source of disorder. Recently researchers have shown a growing interest in a deeper understanding of the effects of fluctuations in biological systems ranging from neuroscience to biological evolution and to population dynamics [1]-[8], [15]-[21].

In addition, analyses of experimental data of population dynamics frequently need to consider spatial heterogeneity. Characterizing the resultant spatio-temporal patterns is, perhaps, the major challenge for ecological time series analysis and for dynamics modeling. To describe complex ecosystems, it is therefore fundamental to understand the interplay between noise, periodic and random modulations of some environment parameters, and the intrinsic nonlinearity of simple models of ecosystems and to understand spatio-temporal dynamics [6, 7],[22]-[26].

The principal aim of this work is to review some recent results obtained for systems described in term of a generalized Lotka-Volterra model including a term of multiplicative noise [1]. A constructive role of the noise is observed. It contributes to producing: (a) quasi-periodic oscillations and stochastic resonance in the presence of a driving force; (b) noise-delayed extinction, (i.e. a nonmonotonic behavior of the average extinction time of one of the two species as a function of the noise intensity); and (c) nonmonotonic behavior of the pattern formation, the density correlation and pattern areas as a function of noise intensity. We analyze three different ecosystems described by the formalism of the Lotka-Volterra equations. The first ecosystem is comprised of two competing species in the presence of two noise sources: a multiplicative noise which affects directly the dynamics of the species, and an additive noise responsible for the random behavior of the interaction parameter between the species. We obtain quasi-periodic oscillations of two species densities, stochastic resonance (SR) and noise-delayed extinction. We also investigate the system using multiplicative colored noise with different values of the correlation time τ_c. The effect of the correlated noise is to shift the peak of the signal-to-noise ratio (SNR), which is the signature of the SR phenomenon. For this ecosystem we also analyzed the spatial effects by considering a discrete time evolution model of the Lotka-Volterra equations with diffusive terms, namely a coupled map lattice (CML), and we analyzed the spatio-temporal patterns of the two species induced by the noise. In the second ecosystem, comprised of three interacting species, namely one predator and two preys, we analyzed the spatio-temporal

behavior of the species densities. We find: (a) noise-induced pattern formation in the coexistence regime, which depends on the initial conditions, (b) oscillating behavior of the site correlation coefficient with an alternation between coexistence and exclusion regime, (c) nonmonotonic behavior of the pattern area as a function of noise intensity. Finally we consider a system comprised of many interacting species. The analytical resolution of the Lotka-Volterra equations is more difficult in the presence of a large number of species. Nevertheless some analytical approximations for the mean field interaction between the species as well as numerical simulations give some insight into the behavior of complex ecosystems [1, 8, 27]. For a large number of interacting species, it is reasonable, as a phenomenological approach, to choose the growth parameter and the interaction parameter at random from given probability distributions. Within this type of representation, the dynamics of coevolving species can be characterized by statistical properties over different realizations of parameter sets. Though the generalized Lotka-Volterra model has been explored in detail [28], it seems that a full characterization, either deterministic or statistical, of the conditions under which a population becomes extinguished or survives in the competition process, has not been achieved [29, 30]. In this last ecosystem, two types of interaction between the species have been considered: (a) mean field interaction, and (b) random interaction. We focused on the statistical properties of the i^{th} population, obtaining the asymptotic behavior of the time integral and the distributions both of the population and the local field, which is the interaction of all species on the i^{th} population. By introducing an approximation for the time integral of the average species concentration $M(t)$ we obtained analytical results for the transient behavior and the asymptotic statistical properties of the time average of the i^{th} population.

2. **Two competing species.** Time evolution of two competing species is obtained within the formalism of the Lotka-Volterra equations [31] in the presence of a multiplicative noise

$$\frac{dx}{dt} = \mu_1\, x\,(\alpha_1 - x - \beta_1(t)y) + x\,\xi_x(t) \tag{1}$$

$$\frac{dy}{dt} = \mu_2\, y\,(\alpha_2 - y - \beta_2(t)x) + y\,\xi_y(t), \tag{2}$$

where $\xi_x(t)$ and $\xi_y(t)$ are statistically independent Gaussian white noises with zero mean and correlation function $\langle \xi_i(t)\xi_j(t')\rangle = \sigma\delta(t-t')\delta_{ij}$ $(i,j = x,y)$. It is known that the real biological systems are affected by random interactions, because of the presence of environmental fluctuations. The noise and some other deterministic periodical driving force present in the ecosystems, such as the temperature, contribute to determine also the dynamics of β, the interaction parameter between the species. For $\beta < 1$ a coexistence regime takes place (that is, both species survives), while for $\beta > 1$ an exclusion regime is established (that is, one of the two species vanishes after a certain time). Coexistence and exclusion of one of the two species correspond to stable states of the Lotka-Volterra's deterministic model [32]. The change in the competition rate between exclusion and coexistence occurs randomly because of the coupling between the limiting resources and the noisy environment. A random variation of limiting resources produces a random competition between the species. The noise therefore, together with the periodic force, determines the crossing from a dynamical regime ($\beta < 1$, coexistence) to the other one ($\beta > 1$,

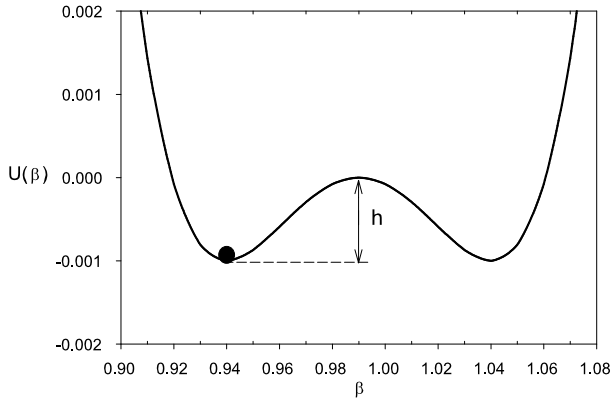

FIGURE 1. The bistable potential $U(\beta)$ of the interaction parameter $\beta(t)$. The potential $U(\beta)$ is centered on $\beta = 0.99$. The parameters of the potential are $h = 6.25 \cdot 10^{-3}$, $\eta = 0.05$, $\rho = -0.01$.

exclusion) [7, 14]. To describe this continuous and noisy behavior of the interaction parameter $\beta(t)$ we consider a stochastic differential equation with a bistable potential and a periodical driving force

$$\frac{d\beta(t)}{dt} = -\frac{dU(\beta)}{d\beta} + \gamma cos(\omega_0 t) + \xi_\beta(t), \tag{3}$$

where $U(\beta)$ is a bistable potential (see Fig. 1)

$$U(\beta) = h(\beta - (1+\rho))^4/\eta^4 - 2h(\beta - (1+\rho))^2/\eta^2, \tag{4}$$

and h is the height of the potential barrier. The periodic term takes into account for the environment temperature variation. Here $\gamma = 10^{-1}$ and $\omega_0/(2\pi) = 10^{-3}$. In Equation (3) $\xi_\beta(t)$ is a Gaussian white noise with the usual statistical properties: $\langle \xi_\beta(t) \rangle = 0$ and $\langle \xi_\beta(t)\xi_\beta(t') \rangle = \sigma_\beta \delta(t - t')$. Due to the shape of $U(\beta)$ it is reasonable to expect a coexistence regime for $\beta(0) < 1$, when deterministic case ($\xi_\beta(t) = 0$) is considered.

2.1. **Stochastic resonance.** First, we investigate the effect of the noise on the time behavior of the species. Since the dynamics of the species strongly depends on the value of the interaction parameter, we initially analyze the time evolution of $\beta(t)$ for different levels of the additive noise σ_β. To obtain the time series for the two species, we set in Equation (2) $\alpha_1 = \alpha_2 = \alpha$, $\beta_1(t) = \beta_2(t) = \beta(t)$. Depending on the value of the multiplicative noise intensity we obtain: (i) a periodical behavior of $\beta(t)$ in the coexistence region (see Fig. 2a); (ii) the same behavior of Fig. 2a, slightly perturbed by the noise (see Fig. 2b); (iii) a quasi-periodical behavior of the interaction parameter jumping between the two values $\beta = 0.94 < 1$ and $\beta = 1.04 > 1$, respectively corresponding to left side well (coexistence regime) and right side well (exclusion regime) of the potential shown in Fig. 1; and finally (iv) a loss of coherence and a dynamical behavior strongly controlled by the noise (Fig. 2d). We note in Fig. 2c synchronization of noise with driving periodical force [10, 11], the typical signature of stochastic resonance that should appear in real ecosystems, because of geological cause and the environmental noise [33]. The

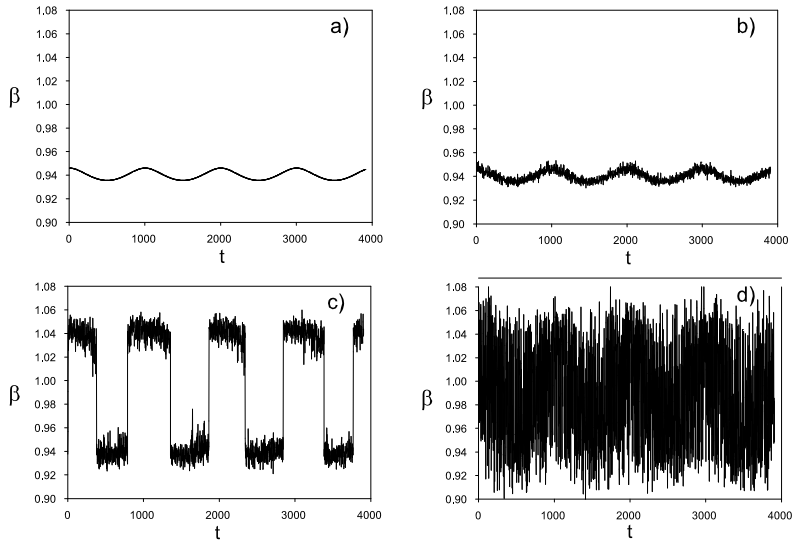

FIGURE 2. Time evolution of the interaction parameter for different values of the additive noise σ_β. (a) $\sigma_\beta = 0$; (b) $\sigma_\beta = 1.78 \cdot 10^{-4}$; (c) $\sigma_\beta = 1.78 \cdot 10^{-3}$; (d) $\sigma_\beta = 1.78 \cdot 10^{-2}$. The values of the parameters are: $\gamma = 10^{-1}$, $\omega_0/(2\pi) = 10^{-3}$.

dynamics of the two species is analyzed by fixing the additive noise intensity at the value $\sigma_\beta = 1.78 \cdot 10^{-3}$, corresponding to a competition regime between the two species periodically switched from coexistence to exclusion. The temporal series of the two species are obtained for different values of the multiplicative noise intensity $\sigma = \sigma_x = \sigma_y$. The initial values of the two species are x(0) = y(0) = 1. In Fig. 3, we report the time series of the two species densities for different values of the multiplicative noise. For $\sigma \sim 0$ (see Figs. 3a), a regime of coexistence with correlated oscillations between the two species is observed. Increasing the intensity of the multiplicative noise anti-correlated oscillations appear characterized by a larger amplitude with periodical random inversions of populations (see Fig. 3b-3c). For higher levels of the multiplicative noise a degradation of the signal and a loss of coherence of the temporal series for the species appears (see Fig. 3d). These series indicate the presence of stochastic resonance (SR): because of a bistable potential modulated by a weak periodic force, the response of the system may be enhanced by the presence of the noise and a periodicity appears. We investigate the presence of SR by considering $(x - y)^2$, the squared difference of population densities. Fig. 4 shows the SNR of this quantity as a function of the multiplicative noise intensity σ, for $\sigma_\beta = 1.78 \cdot 10^{-3}$. We note that dynamics of $(x - y)$ is mainly affected by the multiplicative noise, as we can see from Equations (1), (2). A maximum at $\sigma = 10^{-4}$ is present. The above analysis makes it clear the role of the two noise sources: the additive noise determines the conditions for the different dynamical regimes of the two species, and the multiplicative noise produces a coherent response of the system by a mechanism of symmetry breaking of the dynamical evolution of the ecosystem.

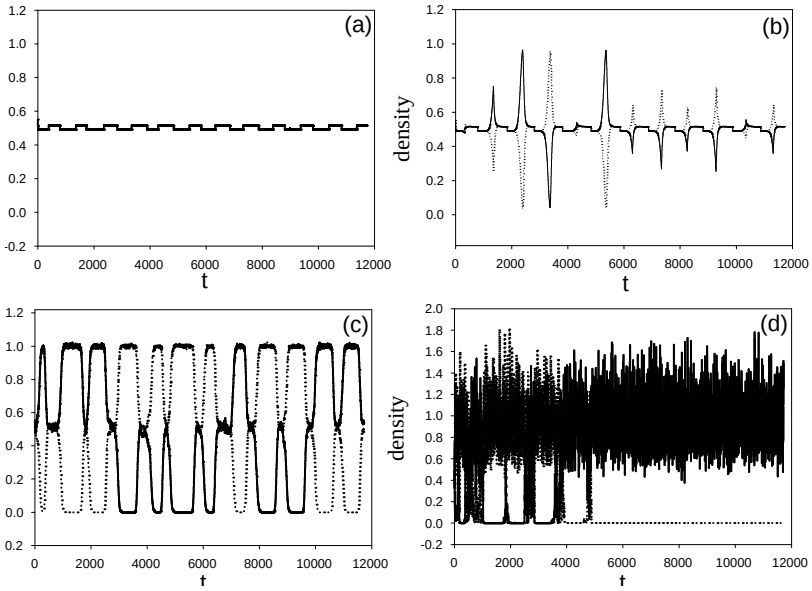

FIGURE 3. Time evolution of both populations at different levels of the multiplicative noise: (a) $\sigma = 0$; (b) $\sigma = 10^{-10}$; (c) $\sigma = 10^{-4}$; (d) $\sigma = 10^{-1}$. The values of the parameters are $\mu = 1$, $\alpha = 1$, $\gamma = 10^{-1}$, $\omega_0/2\pi = 10^{-3}$. The intensity of the additive noise is fixed at the value $\sigma_\beta = 1.78 \cdot 10^{-3}$. The initial values of the two species are $x(0) = y(0) = 1$.

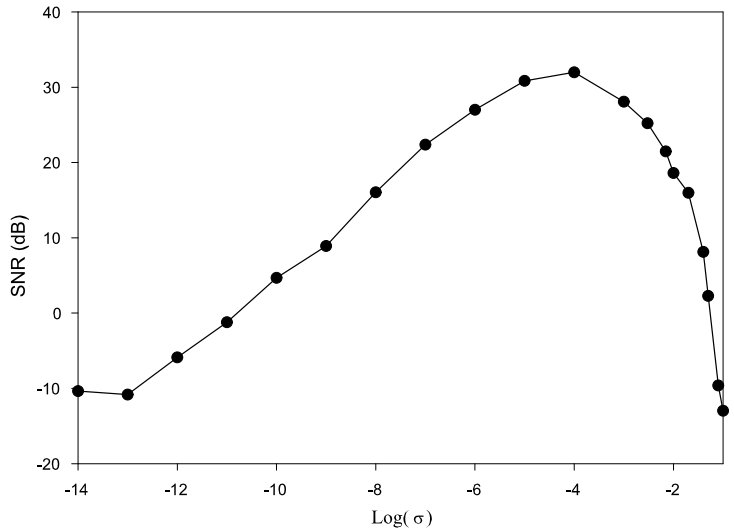

FIGURE 4. Log-Log plot of SNR as a function of the multiplicative noise intensity. The SNR corresponds to the squared difference of population densities $(x-y)^2$. The values of the parameters are the same as Figure 3.

2.2. **Noise-delayed extinction.** We now consider the mean extinction time of one species as a function of the additive noise intensity σ_β, by fixing a low value of multiplicative noise in such a way that the system is far enough from the SR regime [13, 14]. We are not interested in the coherent behavior of the ecological system, but we are focused on the effect of the additive noise on the average extinction time of the species. In Fig. 5 the usual initial condition, $\beta(0) = 0.94$, is fixed. We note that for $\sigma_\beta = 0$ the ecosystem is in the coexistence regime; that is, the deterministic extinction time of both species is infinite. By introducing noise causes exclusion to take place and a finite mean extinction time (MET) appears. By varying the intensity of the additive noise in Equation 3 we obtain, of course, a variation of the average extinction time. The delayed extinction is obtained for noise intensities ranging from the intermediate regime (2 in Fig. 5a) to the coexistence regime obtained with higher values of σ (3 in Fig. 5a). This may mimic the behavior of real ecosystems, where a finite mean extinction time may appear because of the presence of a nonvanishing level of noise intensity. For some environmental reason the noise intensity can change considerably, as is observed in experimental data of populations in a very long time interval [34]. Therefore the dynamical behavior shown in Fig. 5 should explain such physical situations, where the variation of the environmental noise produces a delayed extinction of some population. By increasing the noise intensity we obtain noise-delayed extinction and the average extinction time grows reaching a saturation value, that corresponds to a situation in which the potential barrier is absent. We find nonmonotonic behavior of the MET as a function of the noise intensity σ_β, with a minimum value $\tau_{min} = 40.47$ at $\sigma_\beta = 2.75 \cdot 10^{-3}$, which is of the same order of magnitude of the barrier height h (see Fig. 5a). The Kramers time corresponding to this noise intensity is $\tau_k = 41.6$, which is approximately equal to τ_{min}. This result is due to the noise-driven dynamics. In fact, for a low value of noise intensities, the average time to overcome the potential barrier is very high; that is, Kramers times are long. The ecosystem remains in the coexistence regime for a long time and the extinction time is very large. For noise intensity of the same order of magnitude of the barrier height, the system goes toward the exclusion regime of one of two species, and the average extinction time is approximately equal to the Kramers time. We get the minimum value of MET. For higher values of noise intensity, the Kramers time becomes very small, and the representative point of the β parameter moves between the two minima in a very short time. In this condition the system "sees" the average value of the interaction parameter ($\beta = 0.99$), which gives a coexistence regime. In Figs. 5b, 5c, and 5d we show the time evolution of the ecosystem corresponding to the points 1, 2 and 3 of Fig. 5a. We have a coexistence regime in points 1 and 3 and an exclusion regime in point 2.

2.3. **Colored noise.** In real ecosystems the external random perturbations, because of interaction with the environment, are correlated within a finite correlation time. When the time scale of random fluctuations is larger than the characteristic time scale of the ecosystem the external noise cannot be considered white noise. A strongly correlated noise, for example, emerges as the result of a coarse graining over a hidden set of slow variables [10]. In this section we report the effect of realistic noise in the dynamics of two competing species, and specifically on the SR phenomenon in population dynamics in the presence of exponentially correlated noise. The dynamics of our ecosystem is described by Equations (1), (2), and (3). For low values of the correlation time τ_c, the response of the system coincides with

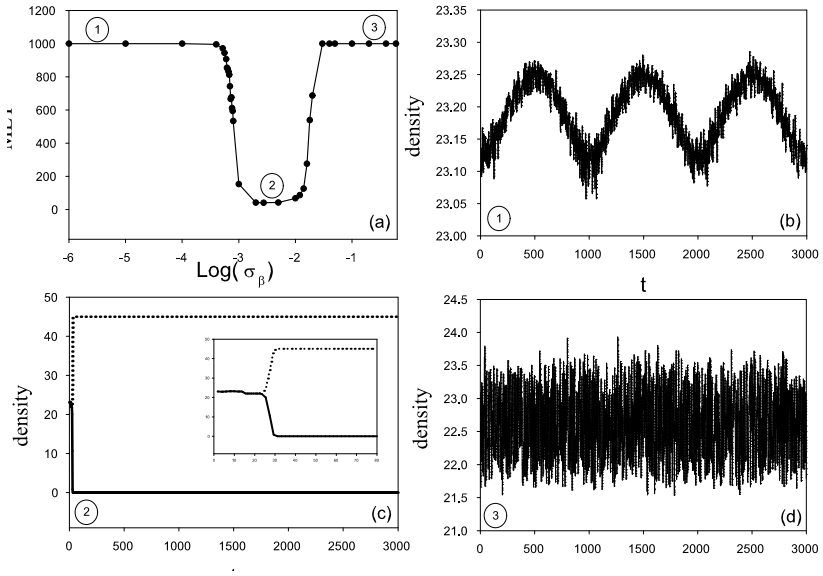

FIGURE 5. (a) Mean extinction time of one species as a function of the noise intensity σ_β. Time evolution of both species for different levels of additive noise: (b) $\sigma_\beta = 10^{-4}$, (c) $\sigma_\beta = 2 \cdot 10^{-3}$, (d) $\sigma_\beta = 10^{-1}$. The values of the parameters are $\mu = 1$, $\alpha = 45$, $\gamma = 10^{-1}$, $\omega_0/2\pi = 10^{-3}$. The intensity of the multiplicative noise is fixed at the value $\sigma = 10^{-9}$. The initial values of the two species are $x(0) = y(0) = 1$.

that obtained with multiplicative white noise. For higher values of τ_c, the coherent response of the system and the maximum of the signal-to-noise ratio (SNR), which are signatures of the SR phenomenon, are shifted towards higher values of the noise intensity. These results agree with previous theoretical and experimental investigations of the SR phenomenon in dynamical systems in the presence of colored noise [10, 35, 36]. However in previous studies the colored noise was additive, while here we have two different sources of noise and only one of them is colored.

Now in Equations (1) and (2), $\xi_i(t)$ $(i = x, y)$ are colored noises given by the archetypal source for colored noise; that is, exponentially correlated processes given by Ornstein-Uhlenbeck process [37]

$$\frac{d\xi_i}{dt} = -\frac{1}{\tau_c}\xi_i + \frac{1}{\tau_c}\eta_i(t) \qquad (i = x, y) \tag{5}$$

and $\eta_i(t)$ $(i = x, y)$ are Gaussian white noises within the Ito scheme with zero mean and correlation function $\langle \eta_i(t)\eta_j(t')\rangle = 2\sigma\delta(t - t')\delta_{ij}$. The correlation function of the processes of Equation (5) is

$$\langle \xi_i(t)\xi_j(t')\rangle = \frac{\sigma}{\tau_c} e^{-|t-t'|/\tau_c}\delta_{ij} \tag{6}$$

and gives $2\delta(t - t')\delta_{ij}$ in the limit $\tau_c \to 0$. Analogous to the previous case (i.e. multiplicative white noise), the time series for the two populations are obtained setting $\alpha_1 = \alpha_2 = \alpha$, $\beta_1(t) = \beta_2(t) = \beta(t)$, and $\xi_x(t) = \xi_y(t) = \xi(t)$, where

the interaction parameter $\beta(t)$ is described by Equations (3), (4). The optimum coherent time behavior of $\beta(t)$ (Fig. 2c), typical of the SR phenomenon, may be used to obtain the time series of the two species densities in the presence of multiplicative colored noise. Therefore we follow a procedure analogous to that applied in the case of multiplicative white noise: we analyze the dynamics of the two species by fixing the additive noise intensity at the value $\sigma_\beta = 1.78 \cdot 10^{-3}$ (see Fig. 2c), and we vary the intensity of the multiplicative colored noise. We obtain the time series of the two species for different values both of the multiplicative noise intensity $\sigma = \sigma_x = \sigma_y$ and the correlation time τ_c [14, 38]. In particular we investigate the system for (a) $\tau_c < T_o$ and (b) $\tau_c > T_o$, with T_o the period of the deterministic driving force. In the weak correlated noise regime (a), no relevant modifications occur in the temporal series of the two species densities in comparison with the case of multiplicative white noise. The time evolution of the two species shows an anticorrelated behavior with quasiperiodical oscillations with a random inversion of the population that predominates over the other one, as in the white noise case. For $\tau_c \simeq T_o$ some modifications occur. In particular for $\tau_c = 2 \cdot 10^3$ the time series of the two species densities show anticorrelated behavior with quasiperiodical oscillations up to $\sigma = 10^{-2}$ (see Fig. 6d); that is, a delay in the coherent output of our ecosystem. This delay will manifest itself in

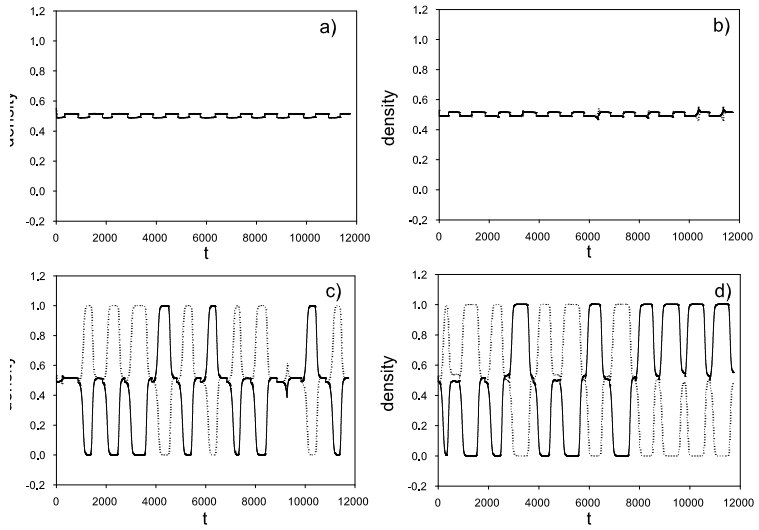

FIGURE 6. Time evolution of both populations at different levels of the multiplicative noise for $\tau_c = 2 \cdot 10^3$: (a) $\sigma = 0$; (b) $\sigma = 10^{-12}$; (c) $\sigma = 10^{-4}$; (d) $\sigma = 10^{-2}$. The values of the parameters are $\mu = 1$, $\alpha = 1$, $\gamma = 10^{-1}$, $\omega_0/(2\pi) = 10^{-3}$. The intensity of the additive noise is fixed at the value $\sigma_\beta = 1.78 \cdot 10^{-3}$. The initial values are: for the two species $x(0) = y(0) = 1$, for the additive (white) noise $\beta(0) = 0.94$, for the multiplicative (colored) noise $\zeta_1(0) = \zeta_2(0) = 0$.

the behavior of the signal-to-noise ratio (SNR) as a function of the multiplicative noise intensity. In the strong correlated noise regime (b), a relevant delay of the

coherent time behavior of the two species is observed. The maximum SNR is shifted toward higher values of the multiplicative noise intensity. This shift in a Log-Log scale grows faster than a linear function of the correlation time τ_c. The coexistence regime and the correlated oscillations of both populations persist for a wider range of multiplicative noise intensities. The anticorrelated behavior with quasiperiodical oscillations appears with very high noise intensity as the correlation time value of the multiplicative noise is strong enough. The loss of coherence in the time behaviors of the two species is observed at very high intensities of the multiplicative noise. Because of the high values of the multiplicative noise, one population extinguishes and the other one survives at a constant density after a transient dynamics. This dynamical behavior is typical of an ecosystem in the presence of an absorbing barrier [1]. According the case of multiplicative noise, to underline the presence of SR, we analyze the squared difference of population densities $(x-y)^2$ for different values of τ_c. In Fig. 7 the SNRs of this quantity

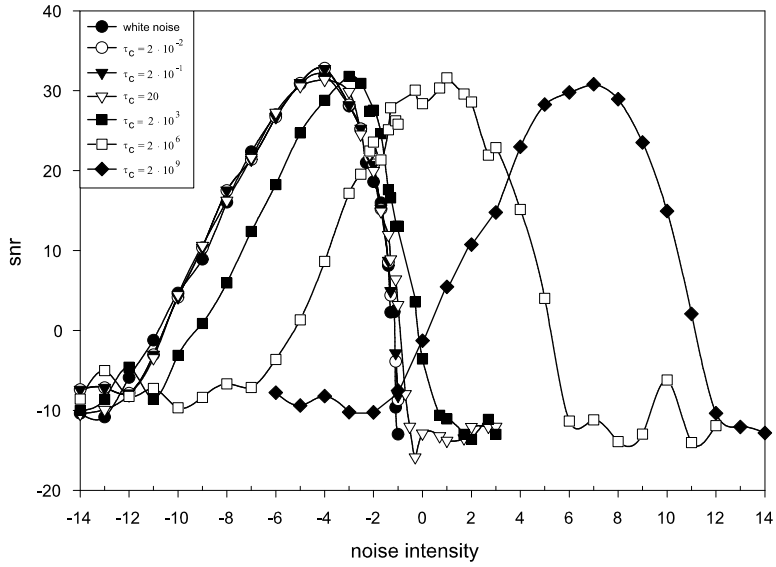

FIGURE 7. Log-Log plot of SNR as a function of noise intensity. The SNR is obtained for six different values of the correlation time: $\tau_c = 2 \cdot 10^{-2}$, $\tau_c = 2 \cdot 10^{-1}$; $\tau_c = 20$; $\tau_c = 2 \cdot 10^3$, $\tau_c = 2 \cdot 10^6$; $\tau_c = 2 \cdot 10^9$. Moreover the signal-noise ratio for white Gaussian noise is reported. The SNR corresponds to the squared difference of population densities $(x-y)^2$. The values of the parameters and the initial condirtions are the same of those used to obtain the temporal series.

are shown for $\tau_c = 0, 2 \cdot 10^{-2}, 2 \cdot 10^{-1}, 20, 2 \cdot 10^3, 2 \cdot 10^6, 2 \cdot 10^9$ as a function of the multiplicative noise intensity σ, by fixing the additive noise intensity [38] at $\sigma_\beta = 1.78 \cdot 10^{-3}$. In each graph of this figure a maximum appears, whose position depends on the values of τ_c; that is, the most coherent response of the system

is connected with both the intensity and the correlation time of the multiplicative noise. We see clearly the two dynamical regimes: (a) weak correlated noise (the first four values of τ_c), (b) strong correlated noise (the last three values of τ_c). In this second regime the maximum SNR is shifted toward higher values of multiplicative noise intensity as in previous theoretical and experimental studies [10, 11, 36]. However some differences occur. Previous studies on the effect of colored noise on the SR phenomenon showed that by increasing τ_c the peak of the SNR shifts toward higher values of the noise amplitude and the maximum decreases with a broadening of the entire curve. The shift of the SR peak to larger noise intensities is due to the fact that colored noise suppresses exponentially the hopping rate with increasing noise color. In our model the colored noise is introduced in the multiplicative noise and not in the additive one as in usual bistable dynamical systems. The SR in the dynamics of the interaction parameter β induces SR phenomenon in the dynamics of two competing populations [14, 38]. Our hopping rate in the first SR is not affected by the *"color"* of the multiplicative noise. However, this noise is responsible for the coherent response of the ecosystem, and therefore the presence of color in the multiplicative noise causes the SNR peak to shift.

2.4. **Spatially extended systems.** To study the spatial effects due to the presence of noise sources we consider a discrete time evolution model, which is the discrete version of the Lotka-Volterra equations with diffusive terms, namely a coupled map lattice (CML) [39]

$$x_{i,j}^{n+1} = \mu x_{i,j}^n(1 - x_{i,j}^n - \beta^n y_{i,j}^n) + \sqrt{\sigma_x} x_{i,j}^n X_{i,j}^n + D\sum_\gamma (x_\gamma^n - x_{i,j}^n), \qquad (7)$$

$$y_{i,j}^{n+1} = \mu y_{i,j}^n(1 - y_{i,j}^n - \beta^n x_{i,j}^n) + \sqrt{\sigma_y} y_{i,j}^n Y_{i,j}^n + D\sum_\gamma (y_\gamma^n - y_{i,j}^n). \qquad (8)$$

In Equations (7) and (8) $x_{i,j}^n$ and $y_{i,j}^n$ denote respectively the densities of species x and species y in the site (i,j) at the time step n, μ is proportional to the growth rate, D is the diffusion constant, $\sum_\gamma$ indicates the sum over the four nearest neighbors. The random terms are white noise sources, modeled by independent Gaussian variables denoted by $X_{i,j}^n$, $Y_{i,j}^n$ with zero mean and variance unit. Here σ_x, σ_y are the intensities of the multiplicative noise that models the interaction between the species and the environment. The interaction parameter β^n of Equations (7) and (8) is a stochastic process which corresponds to the value of continuous $\beta(t)$ of Equation (3) taken at the step n and $\omega_0/2\pi = 10^{-2}$.

We consider the time evolution of the spatial distribution of the ecosystem, described by Equations (7) and (8), in the SR dynamical regime obtained for $\sigma_\beta = 2.65 \cdot 10^{-3}$. We fix the additive noise at this value and vary the intensities of multiplicative noise.

We obtained spatio-temporal patterns of the two species for different values of the multiplicative noise intensity $\sigma = \sigma_x = \sigma_y$, namely $\sigma = 10^{-12}, 10^{-8}, 10^{-4}, 10^{-1}$ with $\mu = 2$, $D = 0.05$, $\gamma = 1.5 \cdot 10^{-1}$, $\omega_0/(2\pi) = 10^{-2}$, $\beta(0) = 0.94$ and $x_{i,j}^0 = y_{i,j}^0 = 0.5$ at all sites (i,j) [40]. For very low noise intensity an average correlation on the considered lattice ($N = 100 \times 100$) between the species is observed. For higher noise intensities an anticorrelation between the two species is observed: the two species tend to occupy different positions. The anticorrelation is more evident for $\sigma = 10^{-4}$ (see Fig. 8a). Increasing the multiplicative noise reduces the anticorrelation strongly (see Fig. 8b).

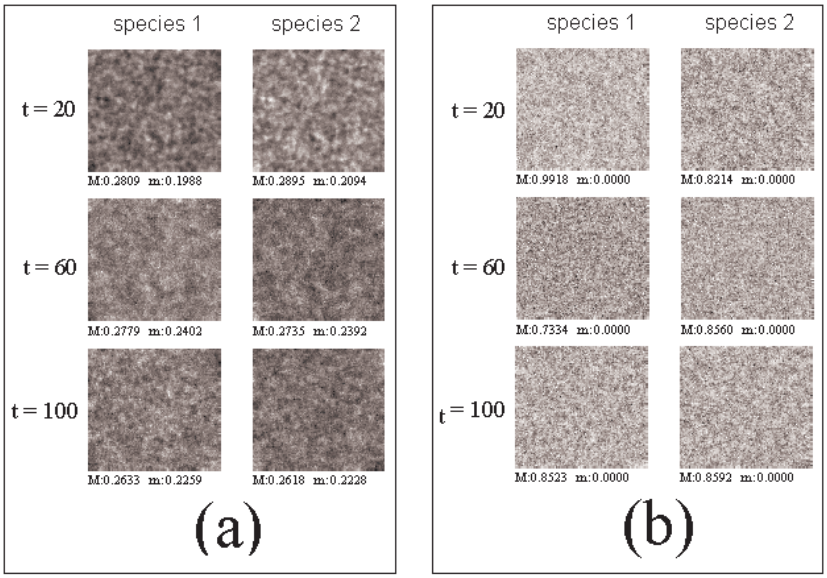

FIGURE 8. Spatial distributions at different times for (a) $\sigma = 10^{-4}$ and (b) $\sigma = 10^{-1}$. The value of the additive noise is fixed at $\sigma_\beta = 2.65 \cdot 10^{-3}$. The values of the parameters are: $\mu = 2$, $D = 0.05$, $\gamma = 1.5 \cdot 10^{-1}$, $\omega_0/(2\pi) = 10^{-2}$, $N = 100 \times 100$. The initial values are $x^0_{i,j} = y^0_{i,j} = 0.5$ for all sites (i, j) and $\beta(0) = 0.94$.

To evaluate the spatial correlation between the two species for the noise intensities considered, we calculate, at the time step n, the correlation coefficient $< c^n >$ defined on the lattice as [40]

$$< c^n >= \frac{cov^n_{xy}}{s^n_x s^n_y} \tag{9}$$

with

$$cov^n_{xy} = \frac{\sum_{i,j}(x^n_{i,j} - \bar{x}^n)(y^n_{i,j} - \bar{y}^n)}{N}, \tag{10}$$

where $\bar{x}^n$, s^n_x, $\bar{y}^n$, s^n_y are the mean value and the root mean square respectively of species 1 and species 2, obtained over the whole spatial grid at the time step n, cov^n_{xy} is the corresponding covariance and $N = 100 \times 100$ the number of sites which compose the grid. The behavior of the correlation coefficient $< c^n >$ as a function of the time for different levels of the multiplicative noise is reported in Fig. 9 [40]. We observe a nonmonotonic behavior of $< c^n >$ as a function of the multiplicative noise intensity. For low noise intensities $\sigma = 10^{-12}$, $< c^n >$ shows weak oscillation around 1, that is strong correlation between the two species. For higher levels of the noise $\sigma = 10^{-10}$, $< c^n >$ is affected by fluctuations and its values vary strongly as a function of the time. A further increase of the multiplicative noise, (i.e., $\sigma = 10^{-8}$ and $\sigma = 10^{-4}$), determines an oscillation of $< c^n >$ around a negative value (i.e., anticorrelation between the two species), with the frequency of the periodical forcing. For higher intensities of the noise $\sigma = 10^{-1}$, the value of

the correlation coefficient $< c^n >$ increases and it vanishes for $\sigma = 10^{+3}$. To show clearly the nonmonotonic behavior of $< c^n >$, we calculate the time average of the correlation coefficient $< c^n >_t$ and we report it, as a function of the multiplicative noise intensity, in Fig. 10. A clear minimum appears, which corresponds to the

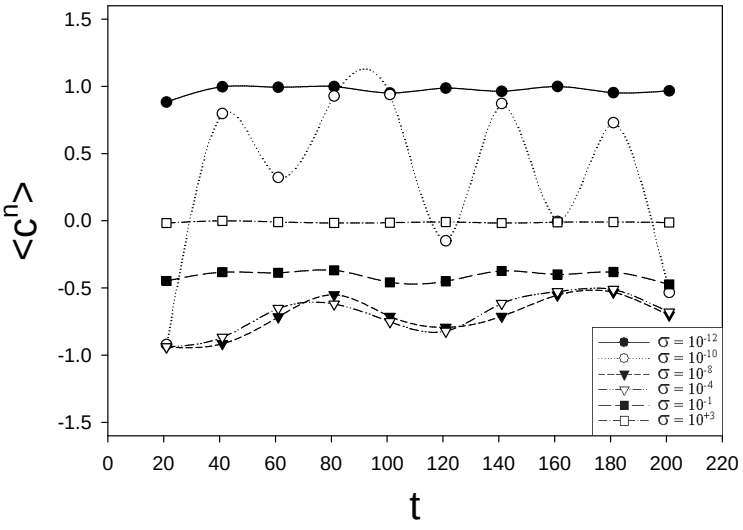

FIGURE 9. Correlation coefficient $< c^n >$ as a function of the time. For low levels of the multiplicative noise ($\sigma = 10^{-12}$) the species are strongly correlated and $< c^n >$ is approximately constant. By increasing the intensity of the multiplicative noise ($\sigma = 10^{-10}$) $< c^n >$ shows big fluctuations. A further increase of the noise ($\sigma = 10^{-8}$, $\sigma = 10^{-4}$) causes strong anticorrelation between the two species with $< c^n >$ oscillating at the frequency of the periodical forcing. For very high levels of noise, the anticorrelation is reduced ($\sigma = 10^{-1}$) and finally it disappears ($\sigma = 10^{+3}$); that is, the species are totally uncorrelated.

anticorrelated oscillations shown in the time evolution of two competing species in each point of our spatial grid. We note therefore the different role of the two noise sources in the ecosystem dynamics. The additive noise determines the conditions of the dynamical regime, the multiplicative noise produces a coherent response of the system [14, 38], which is responsible for the appearance of anticorrelation behavior in the spatial patterns of the species.

3. **Three interacting species.** In this section we report the spatio-temporal dynamics of three interacting species, two preys and one predator, in the presence of multiplicative white noise and a periodical driving force. We use the same coupled map lattice model of the previous section [39]

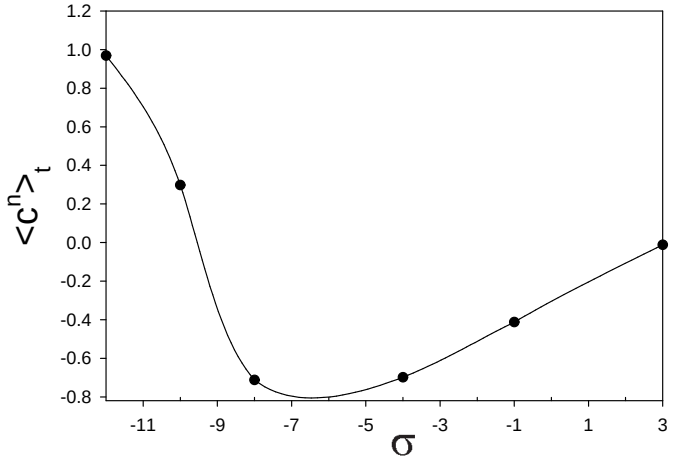

FIGURE 10. Time average of the correlation coefficient $< c^n >_t$ as a function of the multiplicative noise in semilog scale.

$$x_{i,j}^{n+1} = \mu x_{i,j}^n(1-\nu x_{i,j}^n-\beta^n y_{i,j}^n-\gamma z_{i,j}^n)+\sqrt{\sigma_x}x_{i,j}^n X_{i,j}^n+D\sum_\delta(x_\delta^n-x_{i,j}^n), \quad (11)$$

$$y_{i,j}^{n+1} = \mu y_{i,j}^n(1-\nu y_{i,j}^n-\beta^n x_{i,j}^n-\gamma z_{i,j}^n)+\sqrt{\sigma_y}y_{i,j}^n Y_{i,j}^n+D\sum_\delta(y_\delta^n-y_{i,j}^n), \quad (12)$$

$$z_{i,j}^{n+1} = \mu_z z_{i,j}^n[-\beta_z+\gamma_z(x_{i,j}^n+y_{i,j}^n)]+\sqrt{\sigma_z}z_{i,j}^n Z_{i,j}^n+D\sum_\delta(z_\delta^n-z_{i,j}^n), \quad (13)$$

where $x_{i,j}^n$, $y_{i,j}^n$, and $z_{i,j}^n$ are, respectively, the densities of preys x, y and of the predator z in the site *(i,j)* at the time steps n. Here γ and γ_z are the interaction parameters between preys and predator and D is the diffusion coefficient. In previous equations X, Y and Z are the white Gaussian noise variables with

$$\langle X(t)\rangle = \langle Y(t)\rangle = \langle Z(t)\rangle = 0, \quad (14)$$

$$\langle X(t)X(t+\tau)\rangle = \langle Y(t)Y(t+\tau)\rangle = \langle Z(t)Z(t+\tau)\rangle = \delta(\tau), \quad (15)$$

$\sigma_x = \sigma_y = \sigma_z = q$ is the noise intensity, and μ and μ_z are scale factors. $\sum_\delta$ indicates the sum over the four nearest neighbors in the map lattice. The boundary conditions have been established in such a way that no interaction is present out of lattice. The interaction parameter β between the two preys is a periodical function whose value, after n time steps, is given by

$$\beta(t) = 1+\epsilon+\alpha cos(\omega_0 t), \quad (16)$$

with $\epsilon = -0.01$, $\alpha = 0.1$, and $\nu_0 = (\omega_0/2\pi) = 10^{-3}$. The interaction parameter $\beta(t)$ oscillates around the critical value $\beta_c = 1$ in such a way that the dynamical regime of Lotka-Volterra model for two competing species changes from coexistence of the two preys ($\beta < 1$) to exclusion of one of them ($\beta > 1$). We consider two

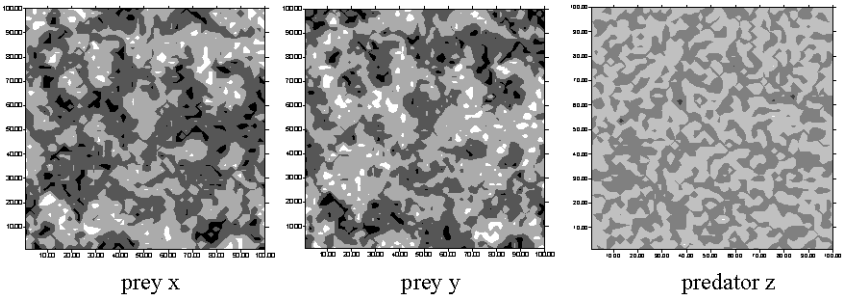

FIGURE 11. Spatial patterns induced by the noise for three interacting species (two preys and one predator) with homogeneous initial distributions. The parameter set is: $\epsilon = -0.01$, $\mu = 2$, $\mu_z = 1$, $\nu = 1$, $\beta_z = 0.01$, $\nu_0 = (\omega_0/2\pi) = 10^{-3}$, $\alpha = 0.1$, $\sigma_x = \sigma_y = \sigma_z = 10^{-8}$, $D = 0.01, \gamma = 3 \cdot 10^{-2}$, $\gamma_z = 2.05 \cdot 10^2$. The initial values of the uniform spatial distribution are $x_{i,j}^{init} = y_{i,j}^{init} = 0.25$ and $z_{i,j}^{init} = 0.10$ for all sites *(i,j)*.

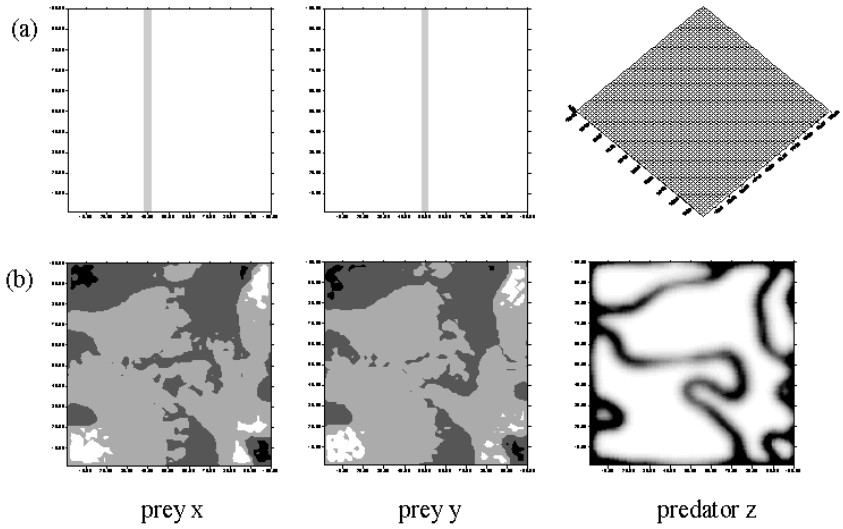

FIGURE 12. Spatial patterns induced by the noise for three interacting species (two preys and one predator) with delta-like initial distributions of the preys and a homogeneous distribution of the predator: (a) initial conditions, (b) spatial patterns after 800 time steps. Here we set $\epsilon = -0.05$, $D = 0.1$, $\sigma_x = \sigma_y = \sigma_z = 10^{-3}$ and the other parameters are the same as in Figure 11.

different initial conditions: (i) a homogeneous initial distribution, and (ii) a peaked initial distribution. In the first case we find exactly anticorrelated spatial patterns of the two preys, while the spatial patterns of the predator show correlations with both the spatial distributions of the preys (see Fig. 11). The preys tend to occupy different positions as in the case of two competing species. In the second case, we use delta-like initial distributions for the two preys and a homogeneous distribution for the predator. After 800 steps we find strongly correlated spatial patterns of

the preys that almost overlap each other. The maximum of spatial distribution of the predator is just at the boundary of the spatial concentrations of the preys, so that the predator surrounds the preys (see Fig. 12). The preys now tend to overlap spatially, as occurs in real ecosystems when preys tend to defend themselves against the predator attacks [13].

The quantitative calculations of the site correlation coefficient between a couple of species in the lattice have been done using the following formula

$$r^n = \frac{\sum_{i,j}^{N}(w_{i,j}^n - \bar{w}^n)(k_{i,j}^n - \bar{k}^n)}{\left[\sum_{i,j}^{N}(w_{i,j}^n - \bar{w}^n)^2 \sum_{i,j}^{N}(k_{i,j}^n - \bar{k}^n)^2\right]^{1/2}} , \tag{17}$$

where N is the number of sites in the grid, the symbols w^n, k^n represent one of the three species x, y, z, and $\bar{w}^n, \bar{k}^n$ represent the mean values of the concentration of the species in all the lattice at the step n. The two-dimensional spatial grid considered is composed by $N = 100 \times 100$ sites in (x, y) plane. The calculations have been done for various noise intensities and at different steps of the iteration process. To quantify our analysis, we consider only the maximum patterns, defined as the ensemble of adjoining sites in the lattice for which the density of the species belongs to the interval $[3/4\ max, max]$, where max is the absolute maximum of density in the specific grid [41]. For each spatial distribution, in a temporal step and for a given noise intensity value, the following quantities have been evaluated referring to the maximum pattern (MP): mean area of the various MPs found in the lattice and spatial correlation r between two preys, and between preys and predator. The parameters used in our simulations are as follows: $\alpha = 0.2$, $\omega_0 = \pi 10^{-3}$, $\epsilon = -0.1$ $\mu = 2$, $\nu = 1$, $\gamma = 0.03$, $\mu_z = 0.02$, $\gamma_z = 205$, and $D = 0.1$. The noise intensity $\sigma_x = \sigma_y = \sigma_z$ varies between 10^{-12} and 10^{-2}.

3.1. **Deterministic analysis.** In the absence of noise and setting constant the value of the interaction parameter β we obtain: (i) for $\epsilon < 0$ ($\beta < 1$) a coexistence regime of the two preys characterized in the lattice by a strong correlation between them with the predator lightly anticorrelated with the two preys; (ii) for $\epsilon > 0$ ($\beta > 1$) wide exclusion zones in the lattice (see Fig. 13), characterized by a strong anticorrelation between preys.

By considering the periodic variation of the interaction parameter $\beta(t)$, we obtain for $\epsilon = 0$, after a transient anticorrelated behavior between preys, a coexistence regime with strong correlation between preys that evolves toward an homogeneous spatial distribution of all three species. For $\epsilon > 0$, we find an oscillating behavior of the site correlation coefficient from coexistence regime between preys (corresponding to strong correlation) to an exclusion regime, corresponding to strong anticorrelation. This last behavior is prevalent. The oscillating frequency coincides with that of the β-parameter. When $\epsilon < 0$, the two preys, after an initial transient, remain strongly correlated for the entire time, despite the fact that the parameter $\beta(t)$ takes values greater than 1 during the periodical evolution. This situation corresponds to a coexistence regime between preys. In Fig. 13, we report the behavior of the site correlation coefficient r as a function of time for three values of the parameter $\epsilon = -0.1, 0, 0.1$ [41].

3.2. **Spatial patterns induced by noise.** To analyze the effect of the noise, we focus on the interesting dynamical regime characterized, in absence of noise, by coexistence between preys in all the period of β that is, with $\epsilon < 0$. The

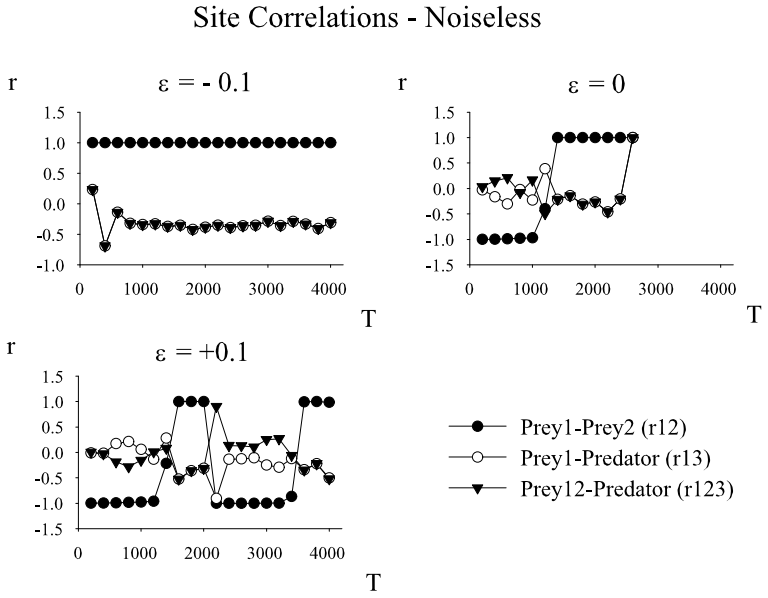

FIGURE 13. Site correlation coefficient r in noiseless dynamics as a function of time for different values of the parameter ϵ : $-0.1, 0., +0.1$. Here $\eta = 0.2$. The parameter set is: $\beta = 1.1, q = 0, D = 0.1, \mu = 2, \nu = 1, \alpha = 0.03, \mu_z = 0.02, \gamma = 205$. The initial conditions are random with a Gaussian distribution, with mean values $\bar{x}(0) = \bar{y}(0) = \bar{z}(0) = 0.25$ and variance $\sigma_o = 0.1$. Here r_{12}, r_{13}, r_{23} and r_{123} are respectively the site correlations between: (i) preys, (ii) prey 1 and predator, (iii) prey 2 and predator, and (iv) predator and both preys.

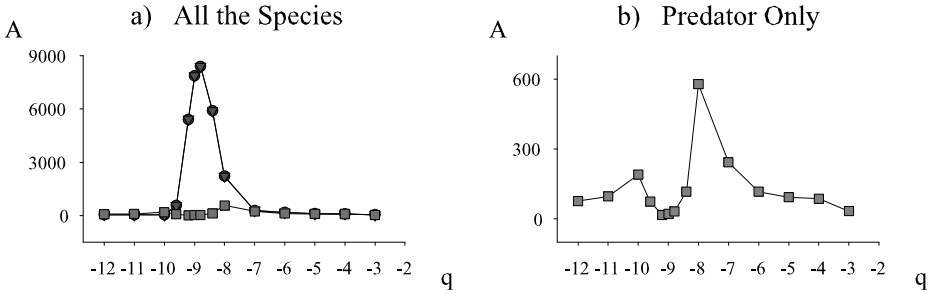

FIGURE 14. Semi-log plot of the mean area of the maximum patterns for all species as a function of noise intensity, at iteration step 1400. Here circles and triangles are related to preys, squares to predator and $\epsilon = -0.1, \eta = 0.2$. The values of the other parameters are the same used for Figure 13. The initial spatial distribution is homogeneous and equal for all species, i.e. $x_{ij}^{init} = y_{ij}^{init} = z_{ij}^{init} = 0.25$ for all sites (i, j).

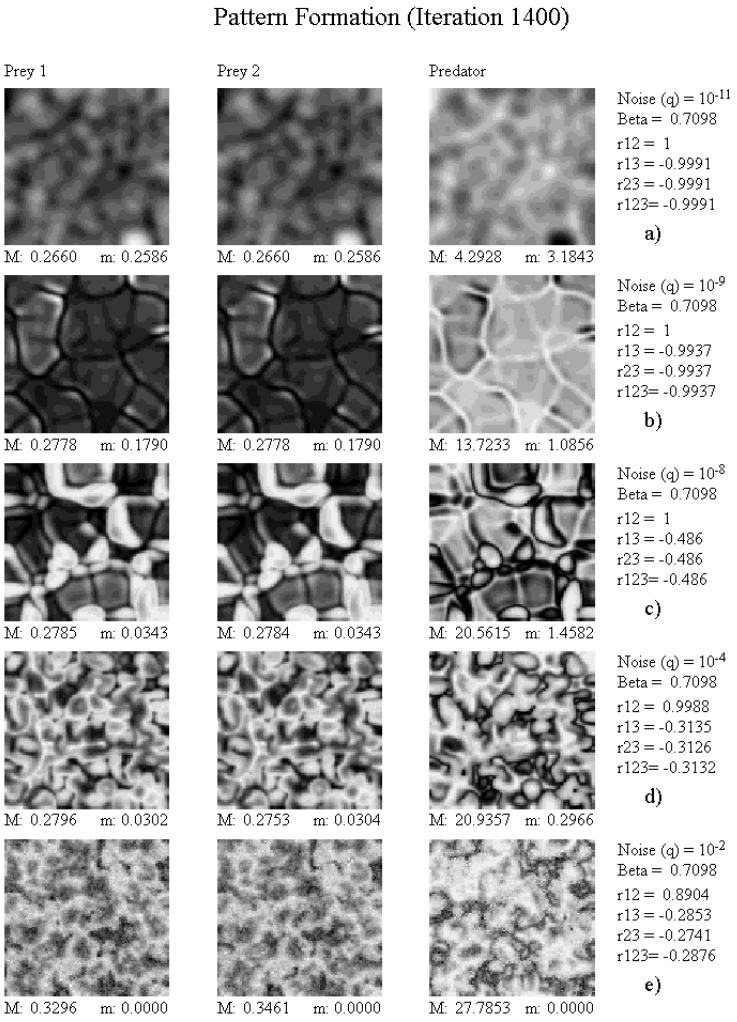

FIGURE 15. Spatial pattern formation for preys and predator, at time iteration 1400 and for the following values of the noise intensity: $q = 10^{-11}, 10^{-9}, 10^{-8}, 10^{-4}, 10^{-2}$. The values of the other parameters and the homogeneous initial distribution are the same used in Figure 14. The parameters $r_{12}, r_{13}, r_{23}, r_{123}$ have the same meaning of Figure 13.

noise triggers the oscillating behavior of the site correlation coefficient r giving rise to periodical alternation of coexistence and exclusion regime. Even a very small amount of noise is able to destroy the coexistence regime periodically. Noise is also responsible for a nonmonotonic behavior of the area of spatial patterns, which repeats periodically in time. In Fig. 14, we report a nonmonotonic behavior of the area of the maximum pattern as a function of noise intensity. A maximum of the area of maximum patterns is visible for the preys at $q = 10^{-9}$ and for the predator

at $q = 10^{-8}$. The same behavior is present in the following time steps within the first period of the interaction parameter: 600, 800, 1200, and 1400. But at time steps 600 and 800 the preys are highly uncorrelated with site correlation coefficient $r_{12} = -1$, while at time steps 1200 and 1400, the preys are highly correlated with $r_{12} = 1$. The formation of spatial patterns appears only when the preys are highly correlated, while large patches with clusterization of preys appear when they are uncorrelated. This means that the coexistence regime between preys corresponds to the appearance of spatial patterns, while the exclusion regime corresponds to clusterization of preys. The noise-induced pattern formation relative to the iteration 1400 is visible in Fig. 15, where we report five patterns of one prey and the predator for the following values of noise intensity: $q = 10^{-11}, 10^{-9}, 10^{-8}, 10^{-4}, 10^{-2}$. The initial spatial distribution is homogeneous and equal for all species; that is, $x_{ij}^{init} = y_{ij}^{init} = z_{ij}^{init} = 0.25$ for all sites (i, j). A spatial structure emerges with increasing noise intensity. This spatial pattern disappears for sufficiently large noise intensity (see Fig. 15e). As a final investigation, we analyze the behavior of the area of the patterns as a function of time. We observe a nonmonotonic behavior of the area of MPs as a function of time for all values of the noise intensity investigated. Particularly for noise intensity values greater than $q = 10^{-7}$, this nonmonotonic behavior becomes periodic in time with the same period of $\beta(t)$, as shown in Fig. 16 for $q = 10^{-4}$. We note that this nonmonotonic behavior doesn't mean that a spatial pattern appears, like that of Fig. 15b, but that a big clusterization of preys density may occur. The maximum at $q = 10^{-4}$ of Fig. 16a in fact corresponds to large patches of preys in the lattice investigated [41]. The various quantities, such as pattern area and correlation coefficient, have been averaged over 200 realizations, obtaining the mean values shown in the Figs. 14 and 16. The effects induced by the

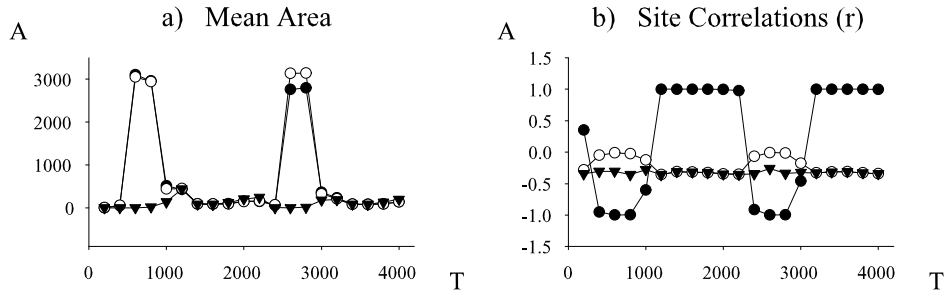

FIGURE 16. Mean area of Maximum pattern of the three species and relative sites correlations between preys and between preys and predator as a function of time and $q = 10^{-4}$. (a): black and white circles are related to preys, triangles to predator; (b) site correlation coefficient r_{12} (black circles), r_{13} (white circles), and r_{123} (triangles). The values of the other parameters and the homogeneous initial distribution are the same used in Figure 13.

multiplicative noise can be summarized as follows: (i) to break the symmetry of the coexistence regime between the preys, producing an alternation with the exclusion regime; (ii) to trigger the oscillating behavior of the site correlation coefficient; and (iii) to produce a nonmonotonic behavior of the pattern area as a function of the noise intensity with an appearance of spatial patterns.

4. **N interacting species.** In the last part of this short review we report the main results obtained by analyzing an ecosystem composed by N interacting species in a noisy environment in the presence of an absorbing barrier; that is, extinction of the species [1, 7, 8].

We consider an N-species generalization of the usual Lotka-Volterra system, and the Ito stochastic differential equation describing the dynamical evolution of the ecosystem is

$$dn_i(t) = \left[\left(\gamma + \frac{\epsilon}{2}\right) - n_i(t) + \sum_{j\neq i} J_{ij} n_j(t)\right] n_i(t)dt + \sqrt{\epsilon} n_i(t) dw_i, \quad i = 1, ..., N \quad (18)$$

where $n_i(t) \geq 0$ is the number of elements of the i^{th} species. In Equation (18), γ is the growth parameter, the interaction matrix J_{ij} modelizes the interaction between different species ($i \neq j$), and w_i is the Wiener process whose increment dw_i satisfies the usual statistical properties

$$< dw_i(t) >= 0; \quad < dw_i(t) dw_j(t') >= \delta_{ij}\delta(t - t')dt. \quad (19)$$

We consider all species equivalent so that the characteristic parameters of the ecosystem are independent of the species. The random interaction with the environment (climate, disease,etc...) is taken into account by introducing a multiplicative noise in the Equation (18). The solution of the dynamical Equation (18) is given by

$$n_i(t) = \frac{n_i(0) exp\left[\delta t + \sqrt{\epsilon} w_i(t) + \int_0^t dt' \sum_{j\neq i} J_{ij} n_j(t')\right]}{1 + \gamma n_i(0) \int_0^t dt' exp\left[\delta t' + \sqrt{\epsilon} w_i(t') + \int_0^{t'} dt'' \sum_{j\neq i} J_{ij} n_j(t'')\right]}. \quad (20)$$

We consider two different types of interaction between the species: (a) a mean field approximation with a symbiotic interaction between the species; (b) a random interaction between the species with different types of mutual interactions: competitive, symbiotic, and prey-predator relationship.

4.1. **Mean field approximation.** We consider a mean field symbiotic interaction between the species. As a consequence, the growth parameter is proportional to the average species concentration,

$$\sum_{j\neq i} J_{ij} n_j(t) = \frac{J}{N} \sum_j n_j(t) = J m(t). \quad (21)$$

In the limit of a large number of interacting species the stochastic evolution of the system is given by the integral equation

$$M(t) = \frac{1}{N} \sum_i \ln\left(1 + n_i(0) \int_0^t dt' e^{JM(t') + \gamma t' + \sqrt{\epsilon} w_i(t')}\right), \quad (22)$$

where $M(t)$ is the time integral of the site population concentration average. We introduce an approximation of this Equation (22) which greatly simplifies the noise affected evolution of the system and allows us to obtain analytical results for the population dynamics. We note that in this approximation the noise influence is taken into account in a nonperturbative way, and that the statistical properties of

the time average process M(t) are determined asymptotically from the statistical properties of the process $w_{max}(t) = \sup_{0<t'<t} w(t')$, where w is the Wiener process. Starting from the following approximated integral equation for $M(t)$

$$M(t) \simeq \frac{1}{N} \sum_i \ln \left(1 + n_i(0) e^{\sqrt{\epsilon} w_{max_i}} \int_0^t dt' e^{JM(t') + \gamma t'} \right), \tag{23}$$

it is possible to analyze the role of the noise on the stability-instability transition in three different regimes of the nonlinear relaxation of the system: (i) toward the equilibrium population ($\gamma > 0$); (ii) toward the absorbing barrier ($\gamma < 0$); (iii) at the critical point ($\gamma = 0$). Specifically at the critical point we obtain for the time average process $M(t)/t$ as a dominant asymptotic behavior in the stability region (namely when $J < 1$)

$$\frac{M(t)}{t} \simeq \left(\frac{1}{1-J} \right) \sqrt{\frac{2\epsilon}{\pi}} \frac{1}{\sqrt{t}}, \tag{24}$$

and in the instability region (namely when $J > 1$)

$$\frac{M(t)}{t} \simeq e^{\langle \ln(n_i(0)) \rangle} \sqrt{\frac{2\pi}{\epsilon}} \frac{e^{\sqrt{\frac{2\epsilon}{\pi}}\sqrt{t}}}{\sqrt{t}} \tag{25}$$

4.2. **Random interaction.** The interaction between the species is assumed to be random and is described by a random interaction matrix J_{ij}, whose elements are independently distributed according to a Gaussian distribution

$$P(J_{ij}) = \frac{1}{\sqrt{2\pi\sigma_J^2}} exp \left[-\frac{J_{ij}^2}{2\sigma_J^2} \right], \ \sigma_J^2 = \frac{J^2}{N}, \tag{26}$$

where J is the interaction strength and

$$< J_{ij} >= 0, \qquad < J_{ij} J_{ji} >= 0. \tag{27}$$

With this asymmetric interaction matrix, our ecosystem contains 50% prey-predator interactions (namely $J_{ij} < 0$ and $J_{ji} > 0$), 25% competitive interactions ($J_{ij} < 0$ and $J_{ji} < 0$), and 25% symbiotic interactions ($J_{ij} > 0$ and $J_{ji} > 0$). The initial values of the populations $n_i(0)$ have also Gaussian distribution

$$P(n) = \frac{1}{\sqrt{2\pi\sigma_n^2}} exp \left[-\frac{(n - < n >)^2}{2\sigma_n^2} \right], \ \sigma_n^2 = 0.01, \text{ and } < n >= 1. \tag{28}$$

The strength of interaction between the species J determines two different dynamical behaviors of the ecosystem. Above a critical value J_c, the system is unstable; this means that at least one of the populations diverges. Below the critical interaction strength, the system is stable and asymptotically reaches an equilibrium state. For our ecosystem this critical value is approximately $J = 1.1$. The equilibrium values of the populations depend both on their initial values and on the interaction matrix. If we consider a quenched random interaction matrix, the ecosystem has a great number of equilibrium configurations, each one with its attraction basin. For vanishing noise ($\epsilon = 0$), the steady state solutions of Equation (18) are obtained by the fixed-point equation

$$(\gamma - n_i + h_i) n_i = 0 \tag{29}$$

where

$$h_i = \sum_j J_{ij} n_j(t) \tag{30}$$

is the local field. For a large number of interacting species, we can assume that the local field h_i is Gaussian with zero mean and variance $\sigma^2_{h_i} =< h_i^2 >= J^2 < n_i^2 >$

$$P(h_i) = \frac{1}{\sqrt{2\pi\sigma^2_{h_i}}} exp\left[-\frac{h_i^2}{2\sigma^2_{h_i}}\right]. \tag{31}$$

The solutions of Equation (29) are

$$n_i = 0, \text{ i. e. extinction} \tag{32}$$

and

$$n_i = (\gamma + h_i)\Theta(\gamma + h_i),\ n_i > 0, \tag{33}$$

where Θ is the Heaviside unit step function. From this equation and applying the self-consistent condition, we can calculate the steady state average population and its variance. Specifically, we have

$$\begin{aligned} < n_i > &= \langle(\gamma + h_i)\Theta(\gamma + h_i)\rangle = \\ &= \frac{1}{\sqrt{2\pi\sigma^2_{h_i}}}\left[\sigma^2_{h_i} exp\left[\frac{\gamma^2}{2\sigma^2_{h_i}}\right] + \frac{\gamma\sqrt{2\sigma^2_{h_i}\pi}}{2}\left(1 + erf\left(\frac{\gamma}{\sqrt{2\sigma^2_{h_i}}}\right)\right)\right], \end{aligned} \tag{34}$$

and

$$\begin{aligned} < n_i^2 > &= \left\langle(\gamma + h_i)^2\Theta^2(\gamma + h_i)\right\rangle = \\ &= \left[\left(\frac{\gamma^2 + \sigma^2_{h_i}}{2}\right)\left(1 + erf\left(\frac{\gamma}{\sqrt{2\sigma^2_{h_i}}}\right)\right) + \frac{\gamma}{2}\sqrt{\frac{2\sigma^2_{h_i}}{\pi}} exp\left[\frac{\gamma^2}{2\sigma^2_{h_i}}\right]\right]. \end{aligned} \tag{35}$$

For an interaction strength $J = 1$ and an intrinsic growth parameter $\gamma = 1$ we obtain: $< n_i >= 1.4387, < n_i^2 >= 4.514$, and $\sigma^2_{n_i} = 2.44$. These values agree with that obtained from numerical simulation of Equation (18). The choice of this particular value for the interaction strength, based on a preliminary investigation on the stability-instability transition of the ecosystem, ensures us that the ecosystem is stable. The stationary probability distribution of the populations is the sum of a delta function and a truncated Gaussian

$$P(n_i) = n_{e_i}\delta(n_i) + \Theta(n_i)\frac{exp\left[-\frac{(n_i - n_{io})^2}{2J^2\sigma^2_{n_i}}\right]}{\sqrt{2\pi J^2\sigma^2_{n_i}}}. \tag{36}$$

The stationary probability distribution of the population densities has been obtained, without the extinct species, in comparison with the computer simulations for systems with N = 1000 species and for an interaction strength $J = 1$, and for $\gamma = 1$ [8].

Now we focus on the statistical properties of the time integral of the i^{th} population $N_i(t)$

$$N_i(t) = \int_0^t dt' n_i(t'), \tag{37}$$

in the asymptotic regime. From Equation (20) we have

$$N_i(t) = \ln \left[1 + n_i(0) \int_0^t dt' exp \left[\gamma t' + \sqrt{\epsilon} w_i(t') + \sum_{J \neq i} J_{ij} N_j(t') \right] \right], \tag{38}$$

In Equation (**??**) the term $\sum_j J_{ij} N_j$ gives the influence of other species on the differential growth rate of the time integral of the i^{th} population and represents a local field acting on the i^{th} population [1, 8, 43]

$$h_i = \sum_j J_{ij} N_j(t) = J\eta_i. \tag{39}$$

We use the same approximation of the Equation (23) and, after differentiating, we get the asymptotic solution of Equation (**??**)

$$N_i(t) \simeq \ln \left[n_i(o) e^{\sqrt{\epsilon} w_{max_i}(t) + J\eta_{max_i}(t)} \int_0^t dt' e^{\gamma t'} \right] \tag{40}$$

where $w_{max_i}(t) = sup_{0<t'<t} w(t')$ and $\eta_{max_i}(t) = sup_{0<t'<t} \eta(t')$. Equation (40) is valid for $\gamma \geq 0$; that is, when the system relaxes toward an equilibrium population and at the critical point. Evaluating Equation (40) for $\gamma \geq 0$, after making the ensemble average, we obtain for the time average of the i^{th} population $\bar{N}_i$

$$\left\langle \bar{N}_i \right\rangle \simeq \frac{1}{t} \left[N_w \sqrt{\epsilon t} + \ln t + \langle \ln [n_i(o)] \rangle \right], \ \gamma = 0, \tag{41}$$

and

$$\left\langle \bar{N}_i \right\rangle \simeq \frac{1}{t} \left[N_w \sqrt{\epsilon t} + (\gamma + N_\eta + \left\langle \ln \left[\frac{n_i(o)}{\gamma} \right] \right\rangle \right], \ \gamma > 0, \tag{42}$$

where N_w and N_η are variables with a semi-Gaussian distribution [1] and N_η must be determined self-consistently from the Equation (39).

These asymptotic behaviors are consistent with those obtained using a mean field approximation. We obtain in fact the typical long time tail behavior ($t^{-1/2}$) dependence, which characterizes nonlinear relaxation regimes when $\gamma \geq 0$. Further, the numerical results confirm these analytical asymptotic behaviors of $\bar{N}_i$ [27].

When the system relaxes toward the absorbing barrier ($\gamma < 0$) we get from Equation (**??**) in the long-time regime

$$\left\langle \bar{N}_i \right\rangle \simeq \frac{1}{t} \left[\ln(n_i(0)) + \ln \left[\int_0^t dt' e^{\gamma t' + \sqrt{t'} w_i(t') + j\eta_i(t')} \right] \right]. \tag{43}$$

In this case the time average of the i^{th} population $\left\langle \bar{N}_i \right\rangle$ is a functional of the local field and the Wiener process, and it depends on the history of these two stochastic processes. We have also analyzed the dynamics of the ecosystem when one species is absent. Specifically, we considered the cavity field, which is the field acting on the

i^{th} population when this population is absent [43]. The probability distributions for both local and cavity field have been obtained by simulations for a time $t = 100$ (expressed in arbitrary units) in absence of external noise, and for two species (namely species 1 and 33) [8]. We found that the probability distributions of the cavity fields differ substantially from those of local fields for the same species unlike the spin glasses dynamics, where the two fields coincide. The same quantities have also been calculated in the presence of the external noise [8]. The effect of the external noise is that the two fields overlap in such a way that for some particular species they coincide. This interesting phenomenon, which is reminiscent of the phase-transition phenomenon, was found for some populations. The main reasons for this peculiar behavior are (i) all the populations are positive; (ii) the particular structure of the attraction basins of our ecosystem; and (iii) the initial conditions, which differ for the value of one population, belong to different attraction basins. Some populations, in the absence of external noise, have a dynamical behavior such that after a long time they significantly influence the dynamics of other species. In the presence of noise, all the populations seem to be equivalent from the dynamical point of view. We also found that for strong noise intensity (namely $\epsilon = 1$) all species extinguish on a long-time scale ($t \approx 10^6$ a. u.). Whether extinction occurs for any value of noise intensity is still an open question, because of time-consuming numerical calculations.

5. **Conclusions.** We briefly reviewed the noise-induced phenomena in population dynamics of three different ecosystems: (i) two competing species, (ii) three interacting species, and (iii) N-interacting species. In the case of two competing species, we considered two sources of white noise: a multiplicative noise and an additive noise, that produces a random interaction parameter between the species. The noise induces a coherent time behavior of two species, giving rise to temporal oscillations and enhancement of the response of the system through the stochastic resonance phenomenon. Specifically the additive noise controls the switching between the coexistence and the exclusion dynamical regimes, the multiplicative noise is responsible for coherent oscillations of the two species. The SR in the dynamics of interaction parameter β induces SR phenomenon in two competing species. These time behaviors are absent in the deterministic dynamics. The noise is also responsible for a delayed extinction that gives rise to a nonmonotonic behavior of the average extinction time as a function of the additive noise intensity. We evaluated the role of colored noise and its effects on the time behavior of the two species. We found that the multiplicative noise is responsible for periodical oscillations of the two species densities, whose amplitude and coherence depend on the value of the correlation time τ_c. For $\tau_c \to 0$ our results are consistent with that obtained for the case of white noise. Moreover the coherent time behavior of our ecosystem and the SR phenomenon are shifted towards higher noise intensities, in agreement with previous theoretical and experimental investigations. We note that our model is useful to describe physical situations in which the amplitude of the periodical driving force, because of the temperature variations, is weak and therefore unable to produce considerable variations of the dynamical regime of the ecosystem. The synergetic cooperation between the nonlinearity of the system and the random and periodical environmental driving forces produces, therefore, a coherent time behavior of the ecosystem investigated. We find that these noise-induced effects should be useful to explain the time evolution of species whose dynamics are strongly affected

by the noisy environment [6, 9, 42, 34]. We also analyzed the role of the noise in spatio-temporal behaviors by using a discrete version of Lotka-Volterra equations with diffusive terms. We found that the noise induces spatio-temporal behaviors that are absent in the deterministic dynamics; that is, pattern formation with the same periodicity of the deterministic force. Moreover appearance of temporal oscillation is observed in the correlation coefficient between the two species and a nonmonotonic behavior of the time-average correlation coefficient as a function of the multiplicative noise.

We also analyzed the role of the noise on the spatio-temporal behaviors of an ecosystem composed by three interacting species. We found that the formation of dynamical spatial patterns occurs with correlations which are strongly dependent on the initial conditions. Moreover, we obtain nonmonotonic behavior of the mean area of the maximum patterns as a function of noise intensity. We find the same behavior for the area of the patterns as a function of evolution time. The noise changes the dynamical regime of the species, breaking the symmetry of the coexistence regime. In addition, the noise produces spatial patterns and temporal oscillations of the site correlation coefficient defined on the lattice. Our model for spatially extended systems composed by two and three species could be useful to explain spatio-temporal behaviors of populations whose dynamics is strongly affected by the noise and by the environmental physical variables; that is, interpreting the experimental data of population dynamics strongly affected by the noise [34, 42]. Finally we analyzed the nonlinear relaxation of an ecosystem composed by N interacting species. By using an approximation of the integral equation, which gives the stochastic evolution of the system, we obtained analytical results that reproduce very well almost all the transient dynamics. We investigated the role of the noise on the stability-instability transition and on the transient dynamics. For random interaction, we obtained asymptotic behavior for three different nonlinear relaxation regimes. We obtain the stationary probability distribution of the population, which is the sum of two contributions: (i) a delta function around $n = 0$ for the extinct species and (ii) a truncated Gaussian for the alive species. When we switch on the external noise, an interesting phenomenon is observed: the local and the cavity fields, whose probability distributions are different in the absence of noise, coincide for some populations. This phenomenon can be ascribed to the peculiarity of the attraction basins of our ecosystem. This model could be useful to describe plankton dynamics.

6. **Acknowledgments.** This work was supported by INFM (Istituto Nazionale per la Fisica della Materia), MIUR (Ministero dell'Istruzione, dell'Università e della Ricerca), and INTAS Grant 01-450 (International Association of the European Community to promote scientific co-operation with New Independent States).

REFERENCES

[1] S. Ciuchi, F. de Pasquale and B. Spagnolo, Phys. Rev. E **53** (1996) 706; F. de Pasquale and B. Spagnolo, *Stochastic Model of Population Dynamics, in Chaos and Noise in Biology and Medicine*, eds. M. Barbi and S. Chillemi, World Scientific **7** Biophysics (1998) 305.
[2] J. M. G. Vilar and R. V. Solé, Phys. Rev. Lett. **80** (1998) 4099.
[3] I. Giardina, J.P. Bouchaud, M. Mezard, J. Phys. A: Math Gen. **34** (2001) L245.
[4] M. Scheffer, et al., Nature **413** (2001) 591.
[5] K. Staliunas, Int. J. of Bifurcation and Chaos **11** (2001) 2845; A. F. Rozenfeld, E. Albano, Physica A **266** (1999) 322; A. F. Rozenfeld *et al.*, Phys. Lett. A **280** (2001) 45.
[6] B. Spagnolo and A. La Barbera, Physica A **315** (2002) 201-211.

[7] B. Spagnolo, M. Cirone, A. La Barbera and F. de Pasquale, Journal of Physics: Condensed Matter **14** (2002) 2247; A. La Barbera and B. Spagnolo, Physica A **314** (2002) 693.
[8] M. A. Cirone, F. de Pasquale and B. Spagnolo, Fractals **11** (2003) 217-226.
[9] See the special section on "Complex Systems", Science **284** (1999) 79-107; C. Zimmer, Science **284** (1999) 83; O. N. Bjornstad and B. T. Grenfell, Science **293** (2001) 638-643.
[10] L. Gammaitoni, P. Hänggi, P. Jung and F. Marchesoni, Rev. Mod. Phys. **70** (1998) 223.
[11] R. N. Mantegna, B. Spagnolo, Phys. Rev. **E49** (1994) R1792; R. N. Mantegna, B. Spagnolo, M. Trapanese, Phys. Rev. **E63** (2001) 011101; E. Lanzara, R. N. Mantegna, B. Spagnolo, R. Zangara, Am. J. Phys. **65** (1997) 341.
[12] N.V. Agudov, B. Spagnolo, Phys. Rev. **E64** (2001) 035102(R); R. N. Mantegna, B. Spagnolo, Phys. Rev. Lett. **76** (1996) 563; R. N. Mantegna, B. Spagnolo, Int. J. Bifurcation and Chaos **8** (1998) 783; A. Fiasconaro, D. Valenti, B. Spagnolo, Physica **A325** (2003) 136; A. Fiasconaro, D. Valenti, B. Spagnolo, Modern Problems of Statistical Physics **2** (2003) 101; N. V. Agudov, A. A. Dubkov, B. Spagnolo, Physica **A325** (2003) 144.
[13] B. Spagnolo, A. Fiasconaro, D. Valenti, Fluctuation and Noise Letters **3** (2003) L177-L185.
[14] D. Valenti, A. Fiasconaro, B. Spagnolo, Physica A **331** (2004) 477-486.
[15] See the special section on "Ecology Through Time", Science **293** (2001) 623-657.
[16] N.Goldenfeld and L.P.Kadanoff, Science **284** (1999) 87.
[17] O. N. Bjornstad et al., Proc. Natl. Acad. Sci. U.S.A. **96** (1999) 5066; K. Higgins et al., Science **276** (1997) 1431.
[18] J. A. Freund, T. Pöschel (Eds.), "Stochastic Processes in Physics, Chemistry, and Biology", Lecture Notes in Physics **557** (2000), Springer, Berlin.
[19] O. N. Bjornstad and B. T. Grenfell, Science **293** (2001) 638-643.
[20] J. H. Brown et al., Science **293** (2001) 643-650.
[21] P. Turchin, L. Oksansen et al., Nature **405** (2000) 562-565.
[22] H. Zhonghuai, Y. Lingfa et al., Phys. Rev. Lett. **81** (1998) 2854-2857 .
[23] D. F. Russel, L. AQ. Wilkens and F. Moss, Nature **402** (2000) 291-294.
[24] A. F. Rozenfeld, C. J. Tessone et al., Phys. Lett. A **280** (2001) 45-52.
[25] A. A. King, W. M. Schaffer, Ecology **82** (2001) 814.
[26] B. Balsius, A. Huppert, L. Stone, Nature **399** (1999) 354.
[27] M. A. Cirone, F. de Pasquale and B. Spagnolo, in Nuclear and Condensed Matter Physics, ed. A. Messina, Vol. **513** (New York: AIP 2000) 365.
[28] Y. M. Svirezhzv and D. O. Logofet, Stability of Biological Communities, (Moscow: Mir 1983).
[29] G. Abramson, Phys. Rev. E **55** (1997) 785.
[30] G. Abramson and D. H. Zanette, Phys. Rev. E **57** (1998) 4572.
[31] A.J. Lotka, Proc. Nat. Acad. Sci. U.S. A. **6** (1920) 410; V. Volterra, Mem. Accad. Nazionale Lincei Ser. 6 **2** (1926) 31.
[32] A. D. Bazykin, Nonlinear Dynamics of Interacting Populations, World Scien. Series on Nonlinear Science, Series A **11** (World Scien. Publishing, Singapore), 1998.
[33] R. Benzi, A. Sutera, A. Vulpiani, J. Phys.: Math Gen. **14** (1981) L453; R. Benzi, G. Parisi, A. Sutera, A. Vulpiani, Tellus **34** (1982) 10; R. Alley, S. Anandakrishnan, P. Jung, Paleoceanogralphy **16** (2001) 190.
[34] A. Caruso, M. Sprovieri, A. Bonanno, R. Sprovieri, Riv. Ital. Paleont. e Strat. **108** (2002) 297; R. Sprovieri, E. Di Stefano, A. Incarbona, M. E. Gargano, "A high-resolution record of the last deglaciation in the Sicily Channel based on foraminifera and calcareous nanofossil quantitative distribution," Palaeogeography, Palaeoclimatology, Palaeoecology (2003) in press.
[35] R. N. Mantegna and B. Spagnolo, Nuovo Cimento D **17** (1995) 873.
[36] P. Hänggi and P. Jung, Adv. Chem. Phys **89** (1995) 239-325.
[37] C. W. Gardiner, Handbook of Stochastic Methods for Physics, Chemistry and the Natural Sciences, 2^{nd} edition, Springer-Verlag, Berlin (1985); W. Horsthemke, R. Lefever, Noise-Induced Transitions, Theory and Applications in Physics, Chemistry and Biology, Springer-Verlag, Berlin (1984).
[38] D. Valenti, A. Fiasconaro, B. Spagnolo, Modern Problems of Statistical Physics **2** (2003) 91-100.

[39] Special issue CML models, edited by K. Kaneko Chaos **2** (1992) 279 ; R. V. Sol et al., J. Theor. Biol. **159** (1992) 469; R. V. Sol et al., Chaos **2** (1992) 387.
[40] D. Valenti, A. Fiasconaro, B. Spagnolo, "Pattern formation and spatial correlation induced by the noise in two competing species," Acta Phys. Pol. B (2004) in press.
[41] A. Fiasconaro, D. Valenti, B. Spagnolo, "Nonmonotonic Behavior of Spatiotemporal Pattern Formation in a Noisy Lotka-Volterra System," Acta Phys. Pol. B (2004) in press.
[42] J. Garcia Lafuente, A. Garcia, S. Mazzola, L. Quintanilla, J. Delgado, A. Cuttitta, B. Patti, Fishery Oceanography **11** (2002) 31-44; S. Mazzola, A. García, and J. García Lafuente, Distribution, biology and biomass estimates of the Sicilian Channel Anchovy, (2000) DG XIV, MED 96-052 Final Report.
[43] M. Mezard, G. Parisi and M. A. Virasoro, Spin Glasses Theory and Beyond (World Scientific Lect. Notes in Physics **9**, Singapore, 1987), 65.

Received on Feb. 1, 2004. Revised on March 12, 2004.

E-mail address: spagnolo@unipa.it